

Polymerization Kinetics and Thermal Properties of Dicyanate/Clay Nanocomposites

Dae Su Kim, Kyung Min Lee

Department of Chemical Engineering, Chungbuk National University San 48, Kaesin-dong, Cheongju, 361-763, Korea

Received 22 April 2003; accepted 17 November 2003

ABSTRACT: The polymerization kinetics and thermal properties of dicyanate/clay nanocomposites were investigated. A type of organically modified clay was used as nanometer-size fillers for the thermosetting dicyanate resin. Differential scanning calorimetry (DSC) was used to study the curing behavior of the dicyanate/clay nanocomposite systems. The polymerization rate of the nanocomposite systems increased with increasing clay content. An autocatalytic reaction mechanism could adequately describe the polymerization kinetics of the dicyanate/clay nanocomposite systems. The polymerization kinetic parameters were deter-

mined by fitting the DSC conversion data to the proposed kinetic equation. The glass-transition temperature of the dicyanate/clay nanocomposites increased with increasing clay content. The thermal decomposition behavior of the dicyanate/clay nanocomposites was investigated by thermogravimetric analysis. © 2004 Wiley Periodicals, Inc. *J Appl Polym Sci* 92: 1955–1960, 2004

Key words: nanocomposites; dicyanate; clay; polymerization kinetics; thermal properties

INTRODUCTION

The mechanical and thermal properties of polymers are generally improved by the addition of inorganic fillers such as silica and talc. High-performance organic–inorganic hybrid materials can be obtained when the interfacial adhesion between the polymer matrix and the reinforcing material is sufficient. Generally, a better interfacial bonding will impart better properties to a polymer composite such as high heat resistance, modulus, tensile strength, and resistance to tear, fatigue, and cracking.^{1,2}

Polymer nanocomposites are a class of composites in which the reinforcing phase dimensions are in the order of nanometers.^{3,4} Because their nanometer-size characteristics maximize the interfacial adhesion, polymer nanocomposites possess superior properties compared to those of conventional polymer microcomposites. Nanostructured composites, based on polymers and layered silicates, typically exhibit properties far superior to those of separate components, which make them extremely interesting in the field of design and creation of new construction materials.⁵ Thus, clays of layered silicates are considered as strong candidates for the preparation of organic–inorganic nanocomposites because they can be broken down into nanometer-scale building blocks, often resulting in optically transparent hybrids. In the last

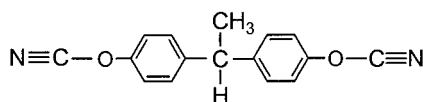
decade, the properties of a variety of elastomers^{6,7} and linear^{8,9} or crosslinked^{10,11} polymers have been improved by the incorporation of layered silicates.

Dicyanate resins are a very useful group of thermoset resins, with mechanical and thermal performance far exceeding that of many commercial epoxy-based systems. Dicyanate resins have advantages in processing because they are low-viscosity resins. Conversion of dicyanate resins to thermosets forms three-dimensional crosslinking networks of oxygen-linked triazine rings and bisphenol units, generally termed polycyanurates. Because no volatile byproducts are formed during curing of dicyanate resins the cyclotrimerization reaction, forming triazine rings, can be classified as a noncondensation-type step polymerization. In general, polycyanurates show high glass-transition temperatures (250–290°C), low water absorption, and good electrical property.¹² Recent studies have focused on their potential matrix applications in advanced polymer composites.^{13–15}

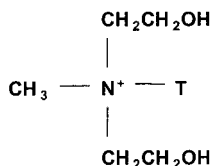
In a previous study,¹⁶ the mechanical properties and nanostructures of the dicyanate/clay nanocomposites were investigated. The mechanical properties of the resin systems were improved by the incorporation of the clay. From the X-ray diffraction (XRD) analysis and the TEM micrographs, it was shown that the silicate layers of clay had been either intercalated to a distance of more than 3 nm or exfoliated in the dicyanate/clay nanocomposites.

To produce high-performance polymer nanocomposites selection of the best curing condition based on the polymerization kinetics is very important. Therefore in this study, the polymerization kinetics and

Correspondence to: D. S. Kim (dskim@chungbuk.ac.kr).



1,1-bis(4-cyanatophenyl) ethane (Arocy L-10)



Methyl tallow bis-2-hydroxyethyl quaternary ammonium (the organic modifier)

Figure 1 Chemical structures of the dicyanate resin and the organic modifier contained in the clay.

thermal properties of dicyanate/clay nanocomposite systems, composed of a low-viscosity dicyanate resin and organically modified clay, were investigated. The effects of clay content within the nanocomposites on the polymerization kinetics were analyzed using the kinetic data obtained by differential scanning calorimetry (DSC). The effects of clay content on the glass-transition behavior and thermal stability of the nanocomposites were also investigated.

EXPERIMENTAL

Materials

The dicyanate resin used in this study was 1,1-bis(4-cyanatophenyl) ethane (Arocy L-10 from Ciba Specialty Chemicals, Summit, NJ). The resin was used as received without further purification. The nanometer-size filler used in this study was a clay, trade name Cloisite 30B, supplied by Southern Clay Products Inc. (Gonzales, TX). The clay is somewhat organophilic because it is treated with an organic modifier, methyl tallow bis-2-hydroxyethyl quaternary ammonium, which is intercalated between silicate layers of clay. Figure 1 shows the chemical structures of the resin and the organic modifier. The T in Figure 1, which means tallow, is composed predominantly of octadecyl chains with smaller amounts of lower homologs (approximate composition: 65% C18, 30% C16, 5% C14). The basal spacing of the organophilic clay was 1.85 nm according to the XRD data supplied by the supplier.

Measurements

DSC

To investigate the curing behavior of the dicyanate/clay nanocomposite systems, a DSC 2910 apparatus

(TA Instruments, New Castle, DE) was used. At room temperature, the organophilic clay was added to the dicyanate resin, and the mixture was stirred rigorously for 1 h to obtain a well-mixed mixture. The mixture was degassed sufficiently in a vacuum oven. About 10 mg of the mixture was placed in a hermetic aluminum sample pan and tested immediately after sealing. The amount of clay in the dicyanate/clay nanocomposites was varied from 0 to 5 phr. Each sample was cured dynamically at different heating rates of 5, 10, and 20°C/min, respectively. The dynamic DSC scans were carried out from room temperature to 350°C under nitrogen gas flow (65 mL/min). After the first scan, the second DSC scan of each fully cured sample was carried out at a heating rate of 10°C/min to monitor the glass-transition behavior of each nanocomposite sample.

Thermogravimetric analysis

Thermogravimetric analysis (TGA) was performed using an SDT 2960 instrument (TA Instruments) to investigate the thermal decomposition behavior of fully cured dicyanate/clay nanocomposites. Each TGA measurement was performed from room temperature to 800°C at a heating rate of 10°C/min under nitrogen gas flow (110 mL/min). Each fully cured sample was prepared by curing the nanocomposite systems dynamically up to 350°C in the DSC sample cell at a heating rate of 10°C/min under nitrogen gas flow (110 mL/min), and then cooling to room temperature.

FTIR

Infrared spectroscopic measurements on the dicyanate/clay nanocomposite systems were performed with the Bomem MB100 FTIR (Bomem Inc., Quebec, Canada) in the wavenumber range of 400–4000 cm^{-1} during isothermal curing at 200°C. The degassed dicyanate/clay mixtures, which are the same as the mixtures prepared for the DSC experiments, were coated on several KBr disks, and placed in an oven that was automatically maintained at 200°C. Each KBr disk was removed from the oven sequentially with a constant time interval, and tested immediately with FTIR to investigate changes in chemical structure during isothermal curing at 200°C.

RESULTS AND DISCUSSION

Figure 2 shows the dynamic DSC thermograms of the dicyanate/clay nanocomposites with various clay contents. The temperature of maximum heat evolution shifted slightly to a lower-temperature region with increasing clay content, and this result means that the polymerization rate of the dicyanate/clay nanocomposite increased slightly as the clay content was in-

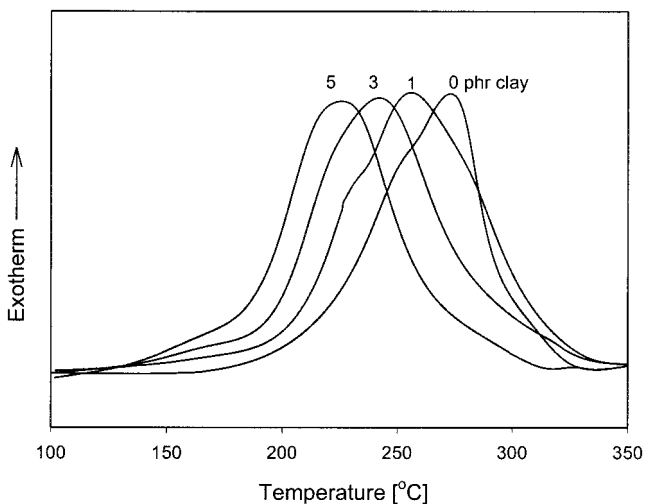


Figure 2 Dynamic DSC thermograms of the dicyanate/clay nanocomposite systems for various clay contents (heating rate = 10°C/min).

creased. Bauer et al.¹⁷ reported that materials containing active hydrogens such as alcohols catalyze the cyclotrimerization reaction of dicyanate resins. The organic modifier, methyl tallow bis-2-hydroxyethyl quaternary ammonium, intercalated between silica layers of the clay used in this study has active hydrogens. Furthermore the surfaces of silicate layers have hydroxyl groups. Thus the polymerization rate of the dicyanate/clay nanocomposites increased with increasing clay content because the active hydrogens in the organic modifier as well as on the surfaces of silicate layers would catalyze the cyclotrimerization reaction of the dicyanate resin.

The curing behavior of dicyanate resins was previously studied by several researchers.^{18–20} They found that the polymerization reaction kinetics of dicyanate resins can be described by a simple second-order Arrhenius-type reaction kinetic equation in the kinetic-controlled regime for catalyzed systems as well as uncatalyzed systems. They used the following second-order autocatalytic reaction kinetic equation to analyze polymerization reaction kinetics of the dicyanate resin systems:

$$\frac{d\alpha}{dt} = (k_1 + k_2\alpha^p)(1 - \alpha)^{2-p} \quad (1)$$

where α is conversion, t is reaction time, and p is the reaction order associated with autocatalytic reaction. The reaction rate constants, k_1 and k_2 , follow an Arrhenius dependency on temperature and are described as follows:

$$k_1 = k_{11}\exp\left(-\frac{E_1}{RT}\right) \quad (2)$$

$$k_2 = k_{22}\exp\left(-\frac{E_2}{RT}\right) \quad (3)$$

where k_{11} and k_{22} are frequency factors, E_1 and E_2 are activation energies for the polymerization reaction, R is the ideal gas constant, and T is absolute temperature.

The autocatalytic reaction kinetic equation, eq. (1) can be expressed as follows by introducing eqs. (2) and (3):

$$\frac{d\alpha}{dT} = \frac{1}{S_r} \left[k_{11}\exp\left(-\frac{E_1}{RT}\right) + k_{22}\exp\left(-\frac{E_2}{RT}\right)\alpha^p \right] (1 - \alpha)^{2-p} \quad (4)$$

where S_r represents the heating rates used in the dynamic DSC measurements.

The dynamic DSC measurements were carried out to supply experimental reaction kinetic data needed in determining the parameters in the reaction kinetic equation [eq. (4)] for the dicyanate/clay nanocomposite systems. The exothermic reaction heats produced during the polymerization reaction of the dicyanate/clay nanocomposite systems were measured by DSC. The chemical conversion was assumed to be the ratio of the partial heat of reaction generated until a certain temperature to the overall heat of reaction at complete conversion ($\alpha = 1$). The experimental conversion data obtained from the dynamic DSC thermograms (Fig. 2) of the dicyanate/clay nanocomposite systems are shown as symbols in Figure 3.

The parameters in the reaction kinetic equation were determined by fitting the kinetic equation [eq. (4)] to the dynamic DSC conversion data through the

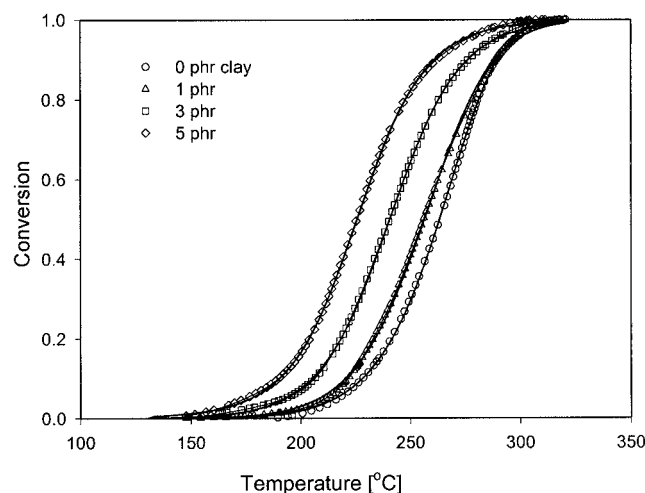


Figure 3 Comparison of conversion changes measured from DSC (points) and calculated from the kinetic model (lines) for the dicyanate/clay nanocomposite systems with various clay contents.

TABLE I
Values of Reaction Kinetic Parameters for the Dicyanate/Clay Nanocomposite Systems Containing Various Amounts of Clay

Clay content (phr)	k_{11} (1/s)	k_{22} (1/s)	E_1 (kJ/mol)	E_2 (kJ/mol)	p
0	7.19×10^5	1.13×10^6	77.4	65.7	0.86
1	2.16×10^{10}	1.25×10^8	109.2	122.6	0.52
3	1.05×10^8	1.43×10^7	87.0	113.0	0.27
5	3.12×10^4	2.38×10^5	55.6	108.8	0.21

Marquardt's multivariable nonlinear regression method and Runge-Kutta integration techniques.²¹ The fitting results are shown in Figure 3 as curves. The experimental conversion data obtained from the dynamic DSC thermograms agree fairly well with the fitting curves calculated from the reaction kinetic equation for the dicyanate/clay nanocomposite systems. The reaction kinetic parameters (k_{11} , k_{22} , E_1 , E_2 , and p) for the dicyanate/clay nanocomposite systems with various clay contents are listed in Table I. The reaction order (p) associated with the autocatalytic reaction was decreased with increasing clay content. It was considered that this result was attributed to the increased catalytic effects of the active hydrogens in the organic modifier as well as on the surfaces of silicate layers with increasing clay content.

Figure 4 shows the DSC thermograms of the dicyanate/clay nanocomposite system containing 5 phr of clay for various heating rates. The temperature of maximum heat evolution increased as the heating rate was increased. The shift of DSC thermograms attributed to an increase of heating rate depends on the activation energy associated with each reaction. Based

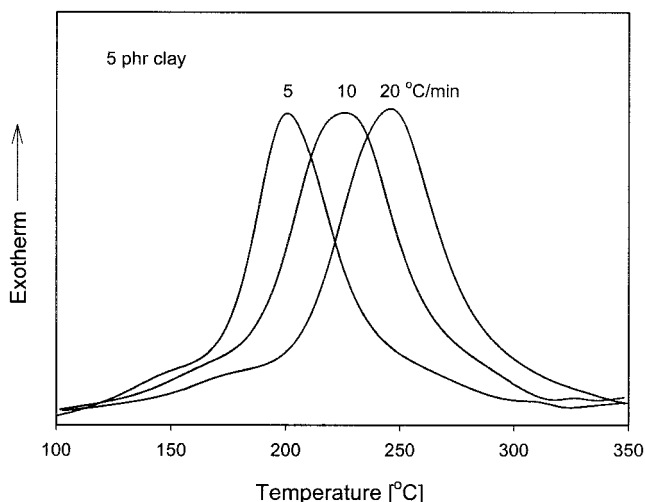


Figure 4 Dynamic DSC thermograms of the nanocomposite system containing 5 phr of clay for various heating rates.

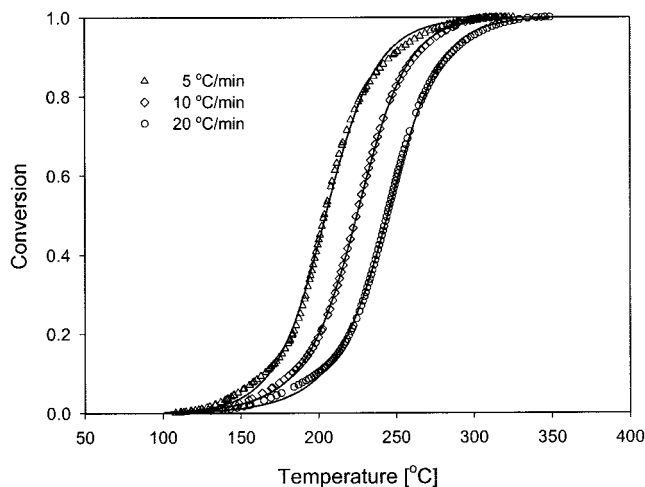


Figure 5 Comparison of conversion changes measured from DSC (points) and calculated from the kinetic model (lines) for various heating rates for the nanocomposite system containing 5 phr of clay.

on this peak-shifting phenomenon, the two simple methods, by Kissinger²² and by Ozawa²³ and Flynn,²⁴ were used to calculate the activation energy associated with each reaction. However, the nonlinear regression method was used in this study to analyze more precisely the reaction kinetics of the dicyanate/clay nanocomposite systems. Figure 5 shows that the experimental conversion data (symbols) obtained from the dynamic DSC thermograms agree well with the conversion curves calculated from the reaction kinetic equation for the dicyanate/clay nanocomposite system containing 5 phr of the clay. The slight deviations of the reaction kinetic model at high conversion range seem to be the result of the diffusion-controlled reaction mechanism of the dicyanate/clay nanocomposite systems after gelation.

Figure 6 shows FTIR spectra showing chemical structure changes occurring during the cyclotrimerization of the dicyanate/clay nanocomposite system containing 5 phr of clay. The peaks for cyanate groups ($-\text{OCN}$) occurring at $2230\text{--}2280\text{ cm}^{-1}$ decreased with reaction time during isothermal curing of the nanocomposite system at 200°C . The peak almost disappeared after 50 min, indicating that the cyclotrimerization reaction was almost finished.

The glass-transition temperatures (T_g 's) of the fully cured dicyanate/clay nanocomposites were measured using DSC at a heating rate of $10^\circ\text{C}/\text{min}$. Figure 7 shows that the T_g of the dicyanate/clay nanocomposites increased as the clay content was increased. This result is reasonable because the polymer chains, possibly intercalated between silicate layers or contacted with exfoliated silicate plates, have less mobility than that of polymer chains in the unfilled systems. The degree of reduced chain mobility would increase with

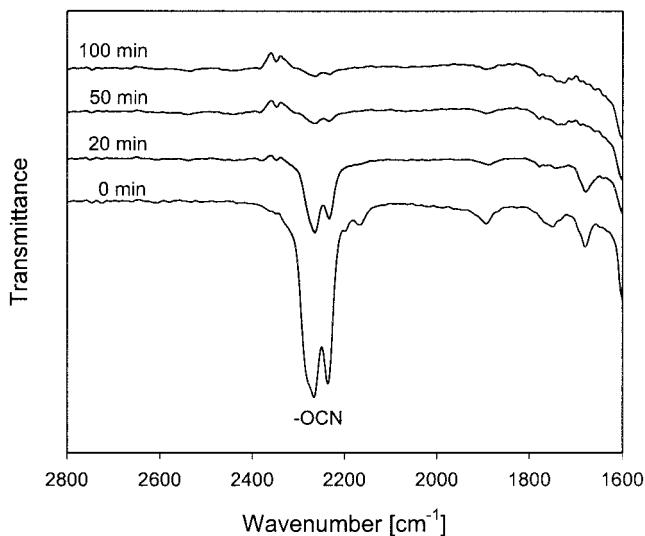


Figure 6 FTIR spectra of the nanocomposite system containing 5 phr of the clay at different curing times during isothermal curing at 200°C.

increasing clay content, and it resulted in an increase of T_g of the dicyanate/clay nanocomposites with increasing clay content.

The thermal decomposition behavior of the fully cured dicyanate/clay nanocomposite with 5 phr of clay was compared with that of the fully cured pure dicyanate resin, as shown in Figure 8. The TGA curves for the nanocomposites containing 1 or 3 phr were observed between the two curves in Figure 8, even though they were not shown in the figure for simplicity. The onset temperature of the thermal decomposition process for the nanocomposite was slightly higher than that for the pure resin system. This result seems

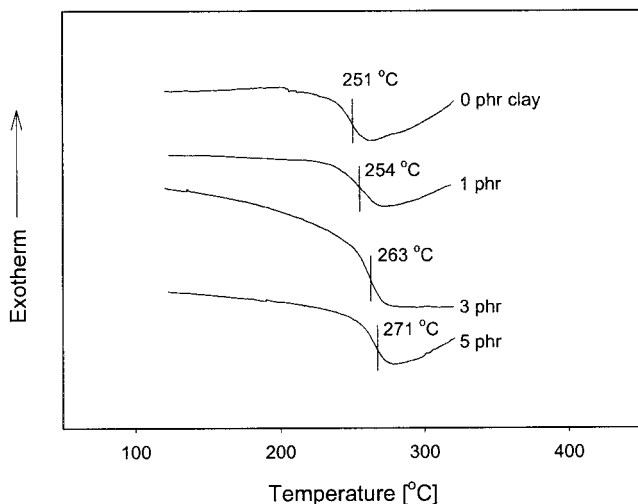


Figure 7 Glass transitions of the dicyanate/clay nanocomposites containing various clay contents (heating rate = 10°C/min).

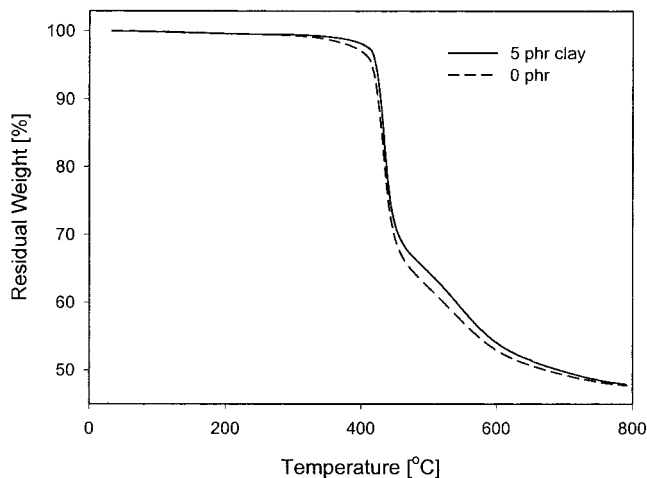


Figure 8 Weight changes of the dicyanate/clay nanocomposites containing various clay contents (heating rate = 10°C/min).

to be caused by both the reduced mobility of the polycyanurate chain network attributed to the introduced clay and the thermally stable inorganic clay itself even though the content is small.

CONCLUSIONS

The effects of changing clay content and dynamic curing condition on the curing behavior and thermal properties of the dicyanate/clay nanocomposite systems were analyzed. The polymerization rate of the dicyanate/clay nanocomposite system increased as the clay content was increased. The reaction kinetics of the dicyanate/clay nanocomposite system could be described fairly well by the second-order autocatalytic reaction kinetic equation. The reaction kinetic parameters were determined from the dynamic DSC conversion data by the fitting method. The glass-transition temperature of the dicyanate/clay nanocomposites increased with increasing clay content. The thermal decomposition process of the dicyanate/clay nanocomposite with 5 phr of clay was slightly hindered compared to the pure dicyanate system.

References

1. Jang, B. Z. *Compos Sci Tech* 1992, 44, 333.
2. Sohn, J. E. *J Adhes* 1985, 15, 19.
3. Novak, B. M. *Adv Mater* 1993, 5, 422.
4. Frisch, H. L.; Mark, J. E. *Chem Mater* 1996, 8, 1735.
5. Giannelis, E. P. *Adv Mater* 1996, 8, 29.
6. Moet, A.; Akelah, A.; Salahuddin, N.; Hiltner, A.; Baer, E. *Mater Res Symp Proc* 1994, 163, 351.
7. Burnside, S.; Giannelis, E. P. *Chem Mater* 1995, 7, 1597.
8. Usuki, A.; Kawasumi, M.; Kojima, Y.; Okada, A.; Kurauchi, T.; Kamigaito, O. *J Mater Res* 1993, 8, 1174.
9. Mehrotra, V.; Giannelis, E. P. *Solid State Ionics* 1992, 51, 115.

10. Lan, T.; Kaviratna, P. D.; Pinnavaia, T. *Chem Mater* 1995, 7, 2144.
11. Akelah, A.; Kelly, P.; Qutubuddin, S.; Moet, A. *Clay Miner* 1994, 29, 169.
12. Shimp, D. A. *SAMPE J* 1987, 19, 41.
13. Papatomas, K. L.; Wang, D. W. *J Appl Polym Sci* 1992, 44, 1267.
14. Osei-Owusu, A.; Martin, G. C.; Groto, J. T. *Polym Eng Sci* 1991, 32, 1604.
15. Zeng, S.; Hoisington, M. H.; Seferis, J. C. *Polym Compos* 1993, 14, 458.
16. Kim, D. S.; Lee, K. M. *J Appl Polym Sci* 2003, 90, 2629.
17. Bauer, M.; Bauer, J.; Kuhn, G. *Acta Polym* 1986, 37, 715.
18. Gupta, A.; Macosko, C. W. *Macromolecules* 1993, 26, 2455.
19. Simon, S. L.; Gillham, J. K.; Shimp, D. A. *Proc ACS Div Polym Mater Sci Eng* 1990, 62, 96.
20. Kamal, M. R.; Sourour, S. *Polym Eng Sci* 1973, 13, 59.
21. Kuester, J. L.; Mize, J. M. *Optimization Techniques with FORTRAN*; McGraw-Hill: New York, 1973.
22. Kissinger, H. E. *Anal Chem* 1957, 29, 1706.
23. Ozawa, T. J. *J Therm Anal* 1976, 9, 217.
24. Flynn, J. H. *Thermochim Acta* 1980, 37, 225.